Volume 88, Number 1 January 2018

Journal of Sedimentary Research

An International Journal of SEPM
(Society for Sedimentary Geology)

Journal of Sedimentary Research

Journal of Sedimentary Research, 2018, v. 88, 24–37
Research Article
DOI: http://dx.doi.org/10.2110/jsr.2017.79

FIELD OBSERVATIONS ON THE EVOLUTION OF RETICULATE PATTERNS IN MICROBIAL MATS IN A MODERN SILICICLASTIC COASTAL ENVIRONMENT

DIANA G. CUADRADO[1,2] AND JERÓNIMO PAN[3,4]

[1]*Instituto Argentino de Oceanografía (IADO, CONICET/UNS), Florida 7500, Bahía Blanca (8000), Provincia Buenos Aires, Argentina*
[2]*Departamento de Geología, Universidad Nacional del Sur, San Juan 670, Bahía Blanca (8000), Provincia Buenos Aires, Argentina*
[3]*Instituto de Investigaciones Marinas y Costeras (IIMyC, CONICET/UNMdP), Rodriguez Peña 4046, Mar del Plata (7600), Provincia Buenos Aires, Argentina*
[4]*Instituto de Geología de Costas y del Cuaternario (UNMdP/CIC), Funes 3350, Mar del Plata (7600), Provincia Buenos Aires, Argentina*
e-mail: cuadrado@criba.edu.ar

ABSTRACT: **Reticulate patterns often found in siliciclastic rocks as wrinkle structures may have been associated with or the product of biological activity. They are also present in modern environments, and laboratory experiments have elucidated the role of filamentous cyanobacteria in their formation, thus considering these microbes putatively as ecosystem engineers. The present study traces the evolution of reticulate structures *in situ* in a modern siliciclastic coastal sedimentary basin for over a year, under different hydrodynamic conditions. The results give new insights on the parameters involved in the formation and preservation of these microbial structures. Field observations documented the development of millimeter-size microbial reticulate structures with specific geometries. They were found in ephemeral ponds starting from two-dimensional submerged laminated cyanobacterial mats, and ultimately created three-dimensional protruding tufts and pinnacles in junctional positions after their desiccation. Reticulate patterns were formed on top of microbial mats four days after a storm flooding and two days after seawater vacated the area under calm conditions, by virtue of the motility of filamentous cyanobacteria. Through their subsequent consolidation they can be maintained in the form of reticulate structures and tufts for extended periods (months). These structures were found sharing an area with deformation sedimentary structures such as microbial folds, roll-ups, and ripped mats, formed under high energy. Therefore, calm settings such as those created by a shallow-water lamina seem to be a requisite for the formation of reticulate structures in the microbial mats, but once they become established, the microbial mats withstand high-energy hydrodynamic regimes. Our observations of modern structures and the sequential *in situ* study of their evolution provide linking references to laboratory and rock-record microbial reticulates, aiding in paleoenvironmental reconstruction.**

INTRODUCTION

Several studies have stated that the reticulate geometries that are often found in siliciclastic rocks as wrinkle structures may be associated with biological activity (Sumner 1997, 2000 and references therein). These morphologies comprise polygonal and elongated bulges over a lower topography where the intersections involve vertically growing microbial filaments forming a tuft texture. Assemblages of microbial polygonal patterns of reticulate ridges with tufted texture have been studied in detail in tidal deposits of Archean age (Sumner 2000; Noffke et al. 2008; Flannery and Walter 2012; Noffke et al. 2013; Homann et al. 2015). Furthermore, complex protruding structures such as tufts and large coniform structures often termed pinnacles have been found extensively in modern environments; e.g., in Laguna Mormona, a hypersaline lagoon in Mexico (Horodyski 1977), the Trucial coast (Park 1977), the Tunisia coast (Gerdes et al. 2000), Yellowstone thermal springs (Petroff et al. 2010), and the Red Sea coastal plain in Saudi Arabia (Taj et al. 2014). Gerdes (2007) extensively documented reticulate patterns, pinnacles (bulges rising some millimeters above the mat surface as the focus of radial bulges), and cyanobacterial filament tufts, both in different field locations and in laboratory-incubated microbial mats. Recent laboratory experiments carried out by Shepard and Sumner (2010) with cultured strains of the cyanobacterium *Pseudanabaena* documented the morphological development of reticulate patterns *in vivo* and attributed the reticulate texture to the undirected motility of filamentous cyanobacteria.

Laboratory (Shepard and Sumner 2010) and geological (Hagadorn and Bottjer 1997; Noffke et al. 2008; Flannery and Walter 2012) studies leave no doubts about the participation of microbial communities on the formation of reticulate and wrinkle structures. Hereinafter, it is important to know the environmental setting and hydrodynamic regime in which the reticulates were formed and developed, and in that sense studies carried out in modern environments are a necessary first step for a proper interpretation of hydrodynamic processes and a detailed reconstruction of paleoenvironments.

Paso Seco (Argentina) is a siliciclastic supratidal flat colonized by thick microbial mats. While these extensive microbial mats would indicate first-hand a low-energy environment, several MISS (microbially induced sedimentary structures *sensu* Noffke et al. 2001) such as microbial chips, flipped-over edges, erosional pockets, and also mat deformation structures (MDS, *sensu* Bouougri and Porada 2012) such as detached mats, microbial folds, and roll-ups, document high-energy flooding events by storm-

Published Online: January 2018
 1527-1404/18/088-024/$03.00

induced high tides (Cuadrado et al. 2015). Certainly, the current velocities may exceed 1.60 m s^{-1}, the critical values measured by Noffke (2010) for erosion stability of epibenthic microbial mats. On the other hand, tidal flooding promotes the formation of high-salinity ephemeral shallow ponds that later dry up. Having recognized the presence of reticulate microbial structures in these ponds, the objective of this study was to trace the evolution of reticulate structures in the field for 21 months, under various environmental conditions. The study documents for the first time the sequential evolution under different energy conditions from two-dimensional submerged laminated cyanobacterial mats in ephemeral ponds, the development of microbial reticulate structures, to the ultimate preservation of pinnacles after desiccation. Thus, our results may contribute to the understanding of environmental cues promoting the establishment of early-Earth microbial-mat communities, and the prevailing paleohydrodynamic conditions during their formation and early preservation.

MATERIAL AND METHODS

This study was based on eight consecutive surveys carried out in the inland coastal area known as Paso Seco (northern Patagonia, Argentina) spanning different seasons. The formation and evolution of surface microbial reticulate structures on this siliciclastic sedimentary plain were sequentially followed along ~ 21 months.

Study Location

Paso Seco (40° 39′ S; 62° 14′ W) is a coastal siliciclastic flat developed on a remnant tidal channel which is currently choked at the mouth by a sand spit formed by NE longshore sediment transport (Espinosa and Isla 2011) (Fig. 1A). The whole sedimentary flat presents episodic flooding during storms (three times per month on average over the last two years), and thus can be considered as a supratidal flat. An elongated area (2.5 km × 0.3 km) is colonized during calm conditions by microorganisms forming thick microbial mats (the uppermost, photosynthetically active layers are on average ± SE = 0.51 ± 0.02 cm; $n = 48$) which generate a smooth and elastic surface. Several stress factors play a role in the environment, such as desiccation over long periods, seasonal water-temperature fluctuations ranging between 7 and 28°C, high salinity (up to 115‰), and several months of groundwater level continuously close to the base level (Fig. 1B, C).

Hydrologic Regime

To detect and record water-level fluctuations in groundwater and by tidal inundation of the sedimentary flat, a water-level logger (HOBO ®, model U20) was placed 40 cm below the flat surface (40° 38′ 1.4″ S; 62° 12′ 23.7″ W). The sensor recorded water level and temperature every 10 min from 5/19/15 to 12/11/15 and from 3/23/16 to 7/7/16, thus producing a 12-month record of flooding (data not shown). Tidal flood currents reach the flats from the NE only under storm conditions, when they are enhanced and pushed by wind and waves, triggering the water to be pushed upward beyond and across the sand spit. In such cases, a maximum 0.7-m water column covers the plain, with a high current shear stress that causes the deformation of the surface microbial mat into roll-ups, folds, and flip-over structures (Cuadrado et al. 2015).

Physical Parameters

Surface sediment temperature, porewater pH and conductivity (when available), and sediment pH and Eh were measured *in situ* at Paso Seco with Hanna Instruments probes (models HI991003 for sediments, HI9033 for water). Sediment samples ($n = 4$) were collected using sawn-off 50 ml medical syringes to obtain sediment cores, and separated into three layers (0–1 cm, 1–3 cm, and 3–6 cm) according to the layered structure visible under a stereoscopic microscope (Nikon SMZ 1500). For each of these layers, total organic matter was calculated from weight loss on ignition after drying samples and ashing at 500°C for 4 h in a muffle furnace (Blakemore et al. 1987).

Biological Sampling and Sample Processing

Different structures were sampled, by removing the surface microbial mat (~ 0.2–0.3 cm) with a sterilized spatula or scalpel. The material was preserved in 5% acidic Lugol's iodine solution (stock solution prepared with natural filtered seawater; Churro et al. 2016), and resuspended into 50 ml with 0.45-μm filtered seawater. In order to disassemble the mat fabric, the sediment cores were homogenized in an ultrasound bath (Testlab®, model TB010). Aliquots were taken from the resuspension, and microorganisms were observed with a compound microscope (Zeiss Axiostar *plus*), at 400×, and relative abundances estimated. Micrographs were taken with an attached digital camera (Canon Powershot A620; Zoom Browser EX 5.5 software). Filamentous cyanobacteria and diatoms were identified to the genus level; the identification of cyanobacteria was based on Waterbury (2006) and Komárek and Hauer (2013); the analysis of diatoms followed Round et al. (1990). Linear dimensions of diameter of a minimum $n = 20$ trichomes (or fascicles in the case of *Microcoleus chthonoplastes* and *Symploca* sp.) were estimated from light micrographs with the online software WebPlotDigitizer v. 3.1, assuming a cylindrical shape of filaments; sheaths were not measured.

Sediment Grain Size

Sediment cores were taken using sawn-off 50-ml medical syringes, and sediment grain size was determined with a laser diffraction particle analyzer Malvern Mastersizer 2000, for particles in the 0.2–2000 μm range, and by sieving for coarser sediments. Organic matter was oxidized before the analysis by adding H_2O_2 with heating and stirring. The statistical parameters used to describe grain-size distribution were calculated with Gradistat software (Blott and Pye 2001).

RESULTS

Sediments and Microbial Mats

The sediment of the tidal plain is composed of siliciclastic minerals (quartz, feldspars, pyroxene; Cuadrado et al. 2015) with grain sizes corresponding mostly to the fine-sand fraction (125–250 μm). Microbial mats were conspicuous both on the surface and at depth as thin organic laminae interspersed with sediments representing multiple generations of biolaminites indicating a continuously growing microbial mat (Fig. 2). The uppermost 3.5-cm sediment profile consisted of microbial mats formed by thin silt layers (40 to 50 μm) randomly separated by sand layers < 0.3 cm thick (Fig. 2B, upper inset). Below these uppermost 3.5 cm, a 5-cm-thick sandy layer was present, containing 0.1–0.3 cm pores. These pores were mostly arranged in a pearl-string pattern (Fig. 2C, lower inset). In the profile, buried microbial mats presented light and dark laminae alternating with thin sand layers below 9 cm depth.

Organic-matter content differed between the upper (0–1 cm) and subjacent (1–6 cm) layers. The upper layer had a 6.01 ± 1.84% wt (average ± SE), whereas the 1–3 cm layer had a 1.66 ± 0.24% wt, and the 3–6 cm layer had a 1.89 ± 0.34% wt. This represents an ~ 3.4-fold increase in organic matter in the uppermost layer, where the mat is living and physiologically active, with respect to the underlying sediment.

Initial Formation of Reticulates

Reticulate microbial structures were first noticed during Austral spring (12 h solar radiance, October 2014), after a typical storm-induced high tide

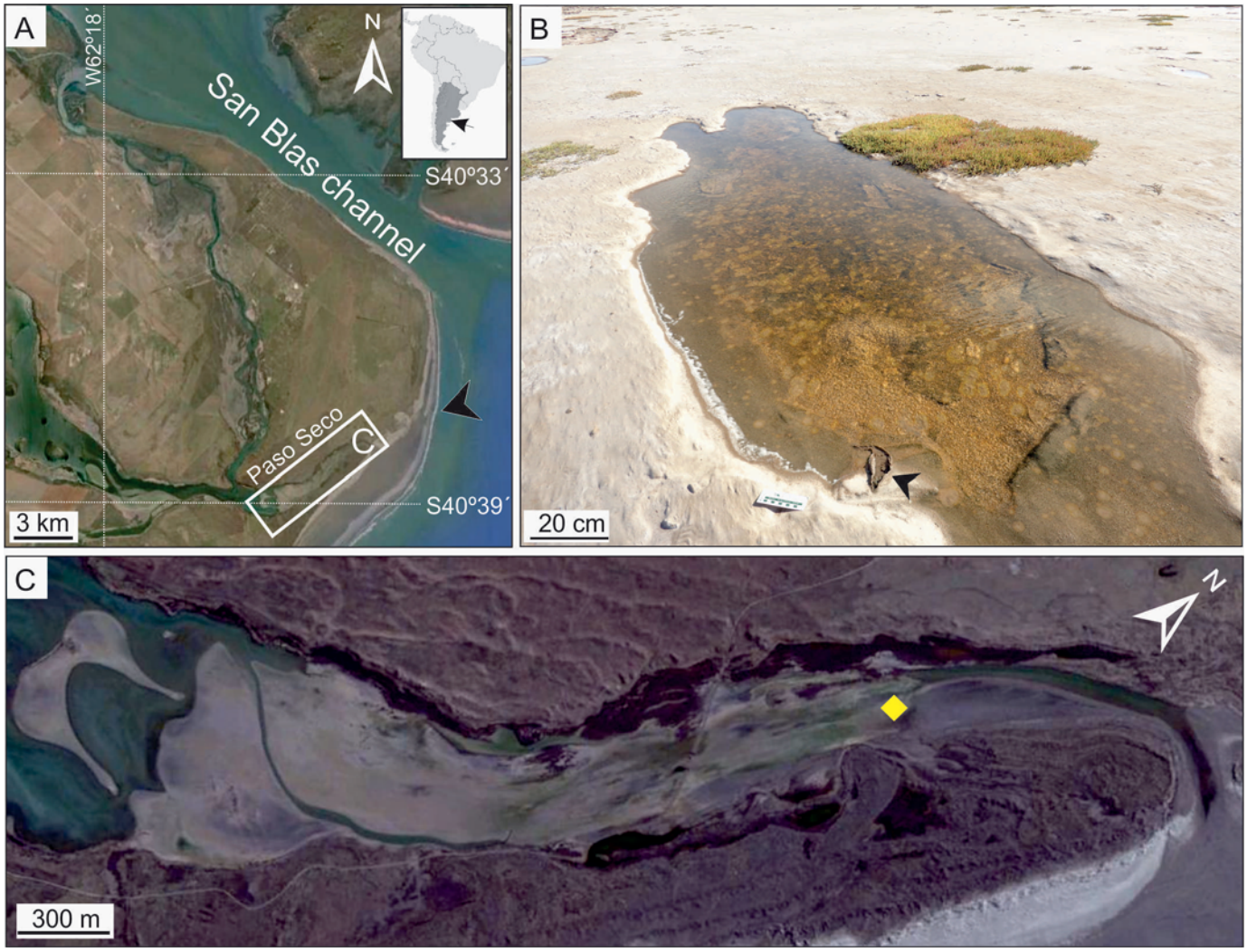

FIG. 1.—**A)** Satellite map showing the inland coastal sedimentary plain at Paso Seco. A connection with the Atlantic Ocean is marked by a black arrow. The inset shows the location of the study area in Part C. **B)** A typical shallow pond colonized by reticulate structures over an established microbial mat. **C)** Coastal plain colonized by thick microbial mats; yellow mark indicates sampling station.

(see location in Fig. 1C). In this occasion the supratidal flat presented elongated erosional pockets where shallow ponds (1–5 cm deep) were formed, remaining wet due to only moderate solar radiation in the spring season (Fig. 1B).

The description of one of the ponds is as follows: the bottom was colonized in patches by a thin layer of blue-green cyanobacteria covered by a light-brown reticulate biofilm (Fig. 3A). The reticulates were formed by 2.5–3.0-mm-wide ridges, uniform along the length and separated 4–5 mm from each other, creating dense polygons (Fig. 3B). Typically, ridges intersect at junctions forming wider structures ($\sim$ 5 mm thick) and high peaks (up to 1 cm in width). The linking of ridges with peaks produces a network with a reticulate geometry.

At the border of the pond, without water, a homogeneous biofilm was present (Fig. 3C), and the substratum below was less visible, although small green patches were noted, implying the presence of cyanobacteria at high densities. The morphology was complex, with several ridges at a higher topography, and the junctions were wider than ridge diameters, forming bulges in some cases. Small bubbles ($<$ 2 mm in diameter) were present under the biofilm, and also perfect circles of the same size can be identified, denoting earlier formation, and burst areas of the pond showed a dense, reticulate pinkish biofilm in conjunction with green zones (Fig. 3D). The pinkish coloration of surface sediments corresponds to carotenoid pigments from Archaea. Positive PCR (polymerase chain reaction) products obtained after amplification of DNA from sediment samples and analyzed with DGGE (denaturing gradient gel electrophoresis) evidenced the presence of Archaea in the plain (not quantified for this study).

One year later, on 10/6/15, in a newly microbial mat, a similar reticulate morphology was found on the same spot of the plain after having been subjected to different hydrodynamic conditions (Fig. 4). On this occasion, five days before the field work, there was 13 mm of precipitation, and one day later the seawater had reached the study area inundating the plain during 30 h with a maximum water column $\sim$ 10 cm; the plain was then exposed to air (for more than 66 h) until the survey (Fig. 4A). The groundwater level during the field survey was 11 cm below the plain. The physicochemical characterization of the water and sediment is presented in Table 1. The air temperature at the cloudy midday was 17°C, and the surface of the plain was mostly wet due to the flood inundation event that took place four days before. It was common to see bulges of different sizes, dark-colored ones (due to presence of the

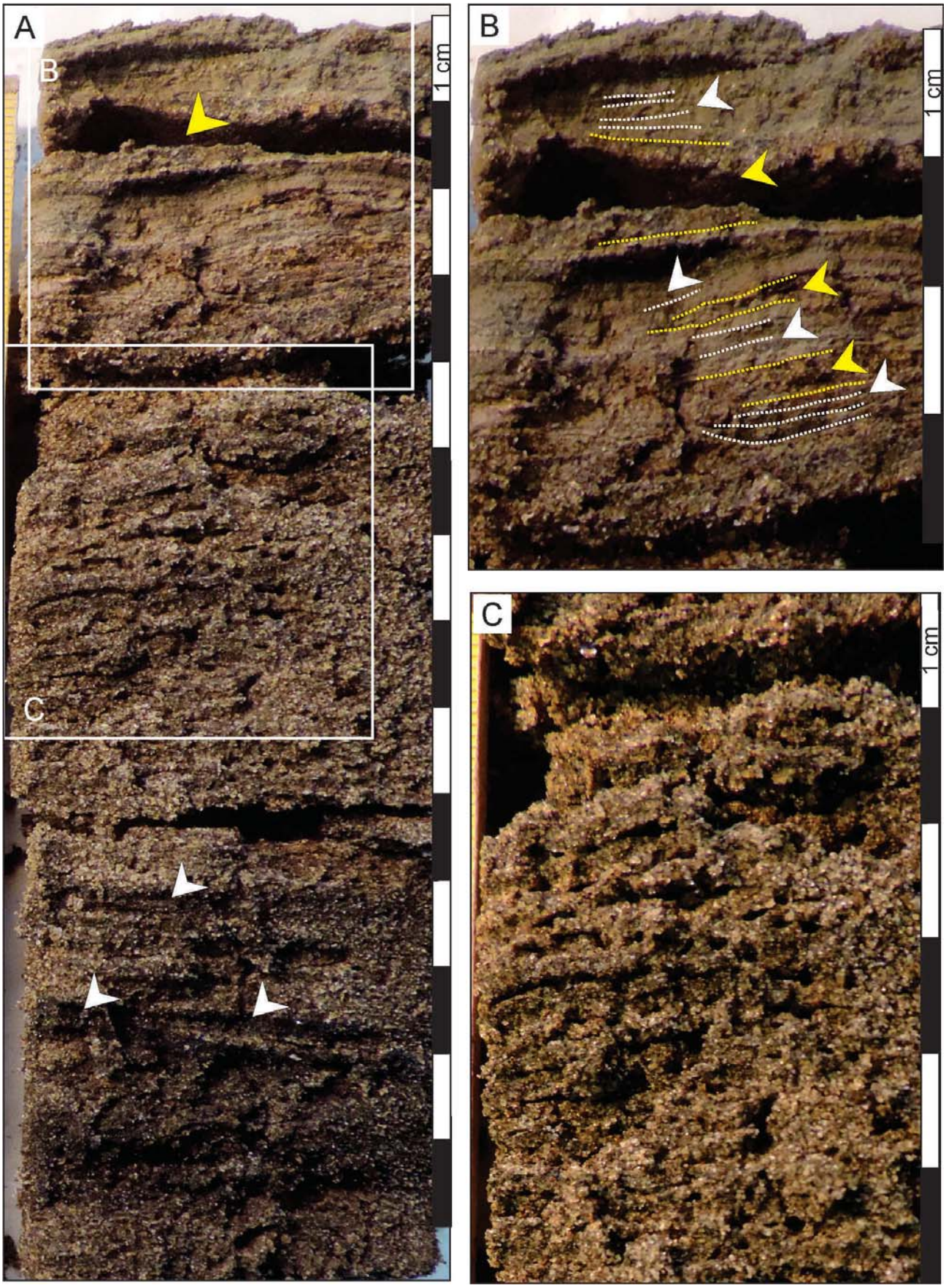
A
B
C
1 cm
B
1 cm
C
1 cm

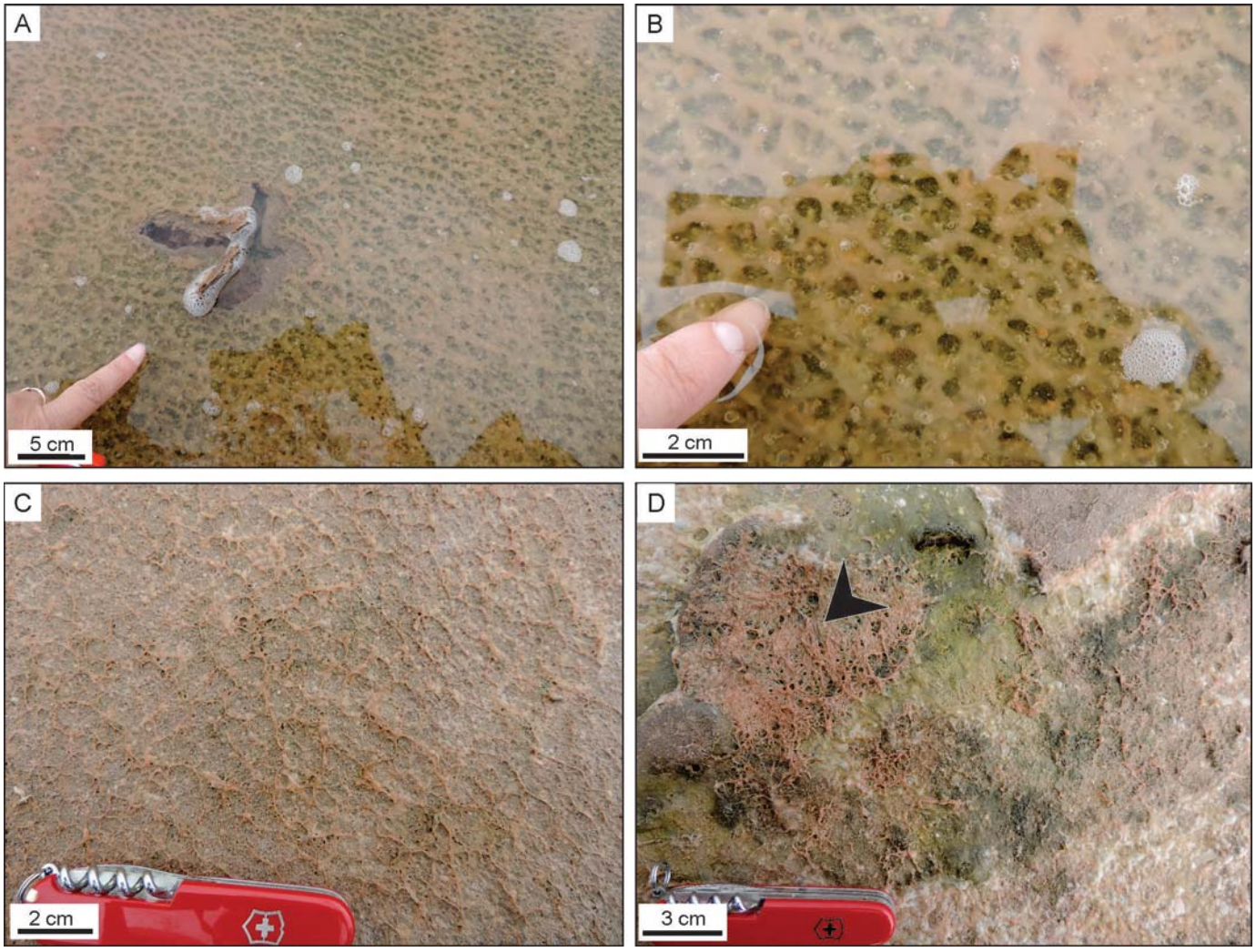

FIG. 3.—Formation of microbial reticulate structures in a pond on top of the microbial mats of Paso Seco, starting with wet conditions (A and B) and ending in the dry-up of the plain (C and D). **A)** Reticulate microbial structures covered by a shallow lamina of water. A greater rhea foot impression broke the surface of the microbial mat showing the underlying sediment (brown). **B)** Close-up view of reticulate structures being wider in the intersections; high-density cyanobacterial patches below are seen as green areas. **C)** Continuous lamina with reticulate structures exposed to air; small interspersed bubbles are on some ridges or on the lamina. **D)** Distinct aspect of the plain surface after the formation of reticulate structures.

cyanobacterium *Calothrix* sp.) and smaller collapsed ones (probably due to gas decay, Fig. 4B). The reticulate morphology presented a pattern similar to that of the previous year, with thick ridges aligned principally in one direction, forming linear patterns, and some bubbles over some ridges (Fig. 4C). The interstitial porewater in this sediment had a pH = 8.18 (Table 1). The underlying mat was green, indicating the presence of cyanobacteria (Fig. 4D). On those spots where the biofilm had a thin sheet of water, it presented a dense aspect (Fig. 4E). A vertical profile from top to bottom consisted of: a brown diatom biofilm, a thin wavy layer of green cyanobacteria, ~ 1–2 mm of several thin, lighter oxic layers, and the underlying black anoxic sediments below with a pH = 5.6 and Eh = –325 mV (Fig. 4F).

The Austral winter survey (July 2016) was carried out after a storm that had lasted 10 days (Fig. 5). The two peaks in the water-level record, reaching a water column of 30 cm over the plain, show the typical storm-induced high tides that inundate the zone frequently (arrows in Fig. 5A). Altogether, the plain was continuously inundated for 22 days, with a stationary 6.5-cm-high water column after the storm. At the time of the field survey, the plain was completely covered by a highly hydrated mucilage, composed of a thick transparent gelatinous diatom biofilm that shielded bubbles of mostly 1–2 mm in diameter, which were interspersed between the sediment and the biofilm exposed to air only after a sharp cutting (Fig. 5B). This gelatinous and coherent biofilm maintained its texture (Fig. 5C). Rhomboidal calcite crystals (shorter diagonal = 39.1 μm;

←

FIG. 2.—**A)** Sediment core showing a vertical profile of the plain with distinct microbial activity. At the top of the core the coherent microbial mat can be seen separating the first 1 cm from the underlying sediment due to a coarser-sand-grain lamina (yellow arrow). The first 3 cm (shown in Part B) is formed by biolaminites of fine sediment over a sandy layer (shown in Part C). Interspersed with the sand, old biolaminites are present (white arrows) implying old microbial-mat colonization. **B)** Close-up view of the surface microbial mat with sedimentary planar lamination, exhibiting laminae of fine sediment (white arrows) intercalated with thin layers of sand (yellow arrows). **C)** Close-up view of the sandy layer that exhibits porous sand, entrapping gases.

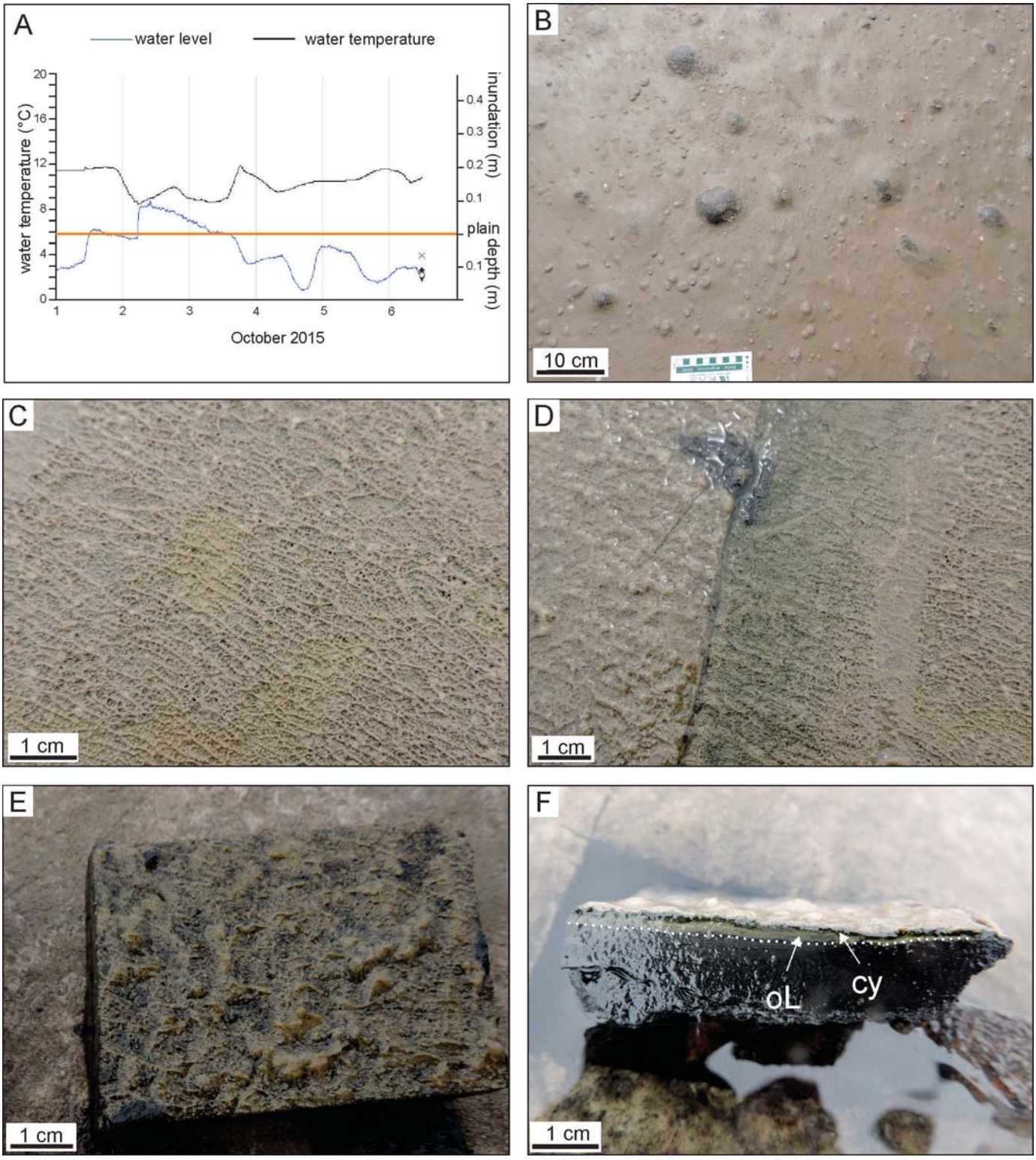

FIG. 4.—**A)** Water temperature and level records for Austral spring from stationary HOBO sensor, previous to a field survey carried out on 10/6/2015; orange line indicates sedimentary-plain ground level. The sharp increase in water level on 10/1/2015 (1 PM) is due to a rain event and the increase on 2/10/2015 indicates the sea-water flooding. **B)** Gas domes present in the microbial mat. **C**, **D)** Surface reticulate structures formed on top of underlying microbial mat; green cyanobacteria-dense patches can be seen under reticulate structures in Part D after a foot trace over the microbial mat. **E**, **F)** Plane view and cross section of more mature reticulate structures developed on top of microbial mat. F) The oxic and anoxic discontinuity is shown (dotted line). Over the oxic layer (oL) a very thin layer of green cyanobacteria (cy) is present.

TABLE 1.—*Physico-chemical parameters of air, porewater, and surface sediment on two sampling dates at Paso Seco.*

	Air	Porewater			Sediment	
Date	Temperature (°C)	Temperature (°C)	Conductivity (mS)	pH	pH	Eh
October 2015 (Austral spring)	17.0	11.6	86.4	7.00	8.18	–3
July 2016 (Austral winter)	14.0	7.7	77.4	7.09	8.00	19

larger diagonal = 60.9 μm) were embedded in the amorphous matrix (Fig. 5D, E). The crystals reacted and were digested with the addition of 10% HCl.

Evolution of Reticulate Patterns

During late Austral summer (15 h solar radiance, March 2015) the study zone was covered by desiccation cracks as a consequence of intense solar radiation; however, the underlying sediment remained wet due to groundwater and capillary ascent (Fig. 6A). One of the common sedimentary structures found in the area were deformed mats developing domes, which are > 8 cm in diameter with a dense darkened appearance on the microbial-mat surface (Fig. 6B, C). On a transverse cut of a dome, the top layer (1–1.5 cm in thickness) presented a deformation at a 40° angle with respect to the bottom layer, and the underlying cavity was filled with fine sand (Fig. 6D). On the surface, the dark desiccated ridges and tufts were similar in appearance to the reticulate structures found in winter. Dark and wide ridges junction formed 1–2 mm-high pinnacles (Fig. 6D–F). In close-up view, the thick and dark ridges developing polygons could be distinguished superimposed on thinner and lighter ridges forming smaller units (Fig. 6E, F). In a transverse-cut view of the pinnacles (Fig. 7A, B) the inner structure could be described as thin green laminae (cyanobacteria) separating light layers of fine sediments (~ 150 μm). The pinnacle was formed by aggregation of filamentous cyanobacteria (see below), covered by evaporitic crystals, probably halite, common in the area after the evaporation of sea water.

Microbial Assemblages

In all cases, non-heterocystous oscillatorian cyanobacteria dominated microbial structures in the biomass, and associated diatoms (mostly pennates) that were largely entangled within the "fabric" of interwoven filaments and embedded in slime EPS (extracellular polymeric substances). Microbial assemblages not only differed macroscopically in their degree of cohesiveness and compaction, but also they differed microscopically on their community composition. The layered microbial mat was very cohesive and hard to disaggregate, despite subjecting the preserved samples to ultrasound and vigorous shaking. The microbial biomass in this mat was dominated by *M. chthonoplastes*, followed by *Lyngbya* sp. (Fig. 8A, B). These two taxa consist of thick filaments with firm sheaths, and they have much larger biomass compared to other morphotypes. The trichomes of *Lyngbya* are on average ~ 2.3 times thicker in diameter than *Pseudanabaena*, while the fascicle of interwoven filaments of *M. chthonoplastes* are ~ 4.4 times thicker than individual *Pseudanabaena* trichomes (Table 2). The *M. chthonoplastes* create a high-density filament mesh. There were other filamentous cyanobacteria contributing less biomass and playing a minor role in conferring structural cohesion, such as *Oscillatoria* sp., *Arthrospira* sp., *Pseudanabaena* sp., *Phormidium* sp., and *Geitlerinema* sp. (Fig. 8C–G). Due to their lower density in relation to

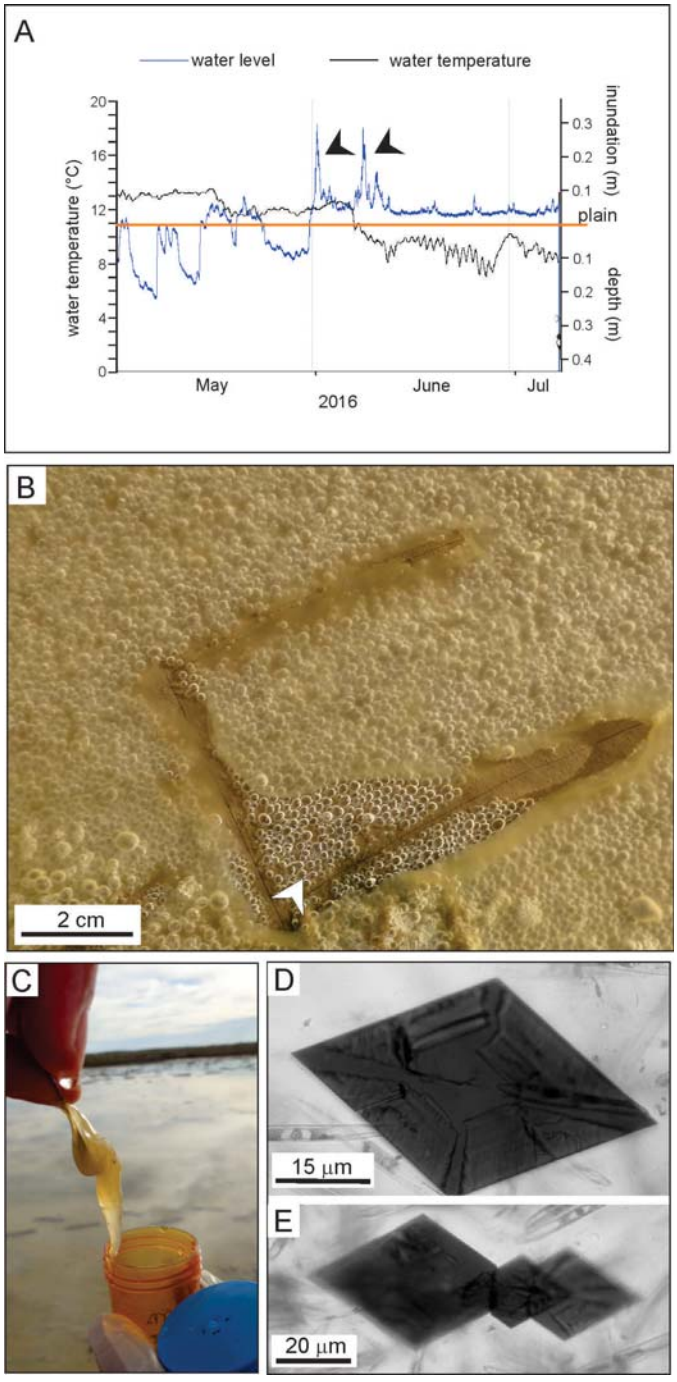

FIG. 5.—**A)** Water temperature and level record for Austral winter from stationary HOBO sensor, previous to a field survey carried out on 7/7/2016; orange line indicates sedimentary-plain ground level. The tidal inundations are shown with arrows. **B)** Substrate covered by a thick gelatinous biofilm. Bubbles produced by cyanobacteria photosynthesis were entrapped below the biofilm and over the microbial mat. An incision of the coherent biofilm exposed the bubbles, which were above the sediment (arrow). **C)** Gelatinous layer covering the plain on 7/7/16. **D**, **E)** Calcite crystals formed in hydrated gelatinous mucilage.

that of *M. chthonoplastes* and *Lyngbya* sp., these could be considered "accessorial" to the mat. Other components of the community were pennate diatoms, such as naviculoids, *Nitzschia sigma*, *Cymatosira belgica*, *Diploneis didyma*, *D. interrupta*, and *Amphora* sp. Centric

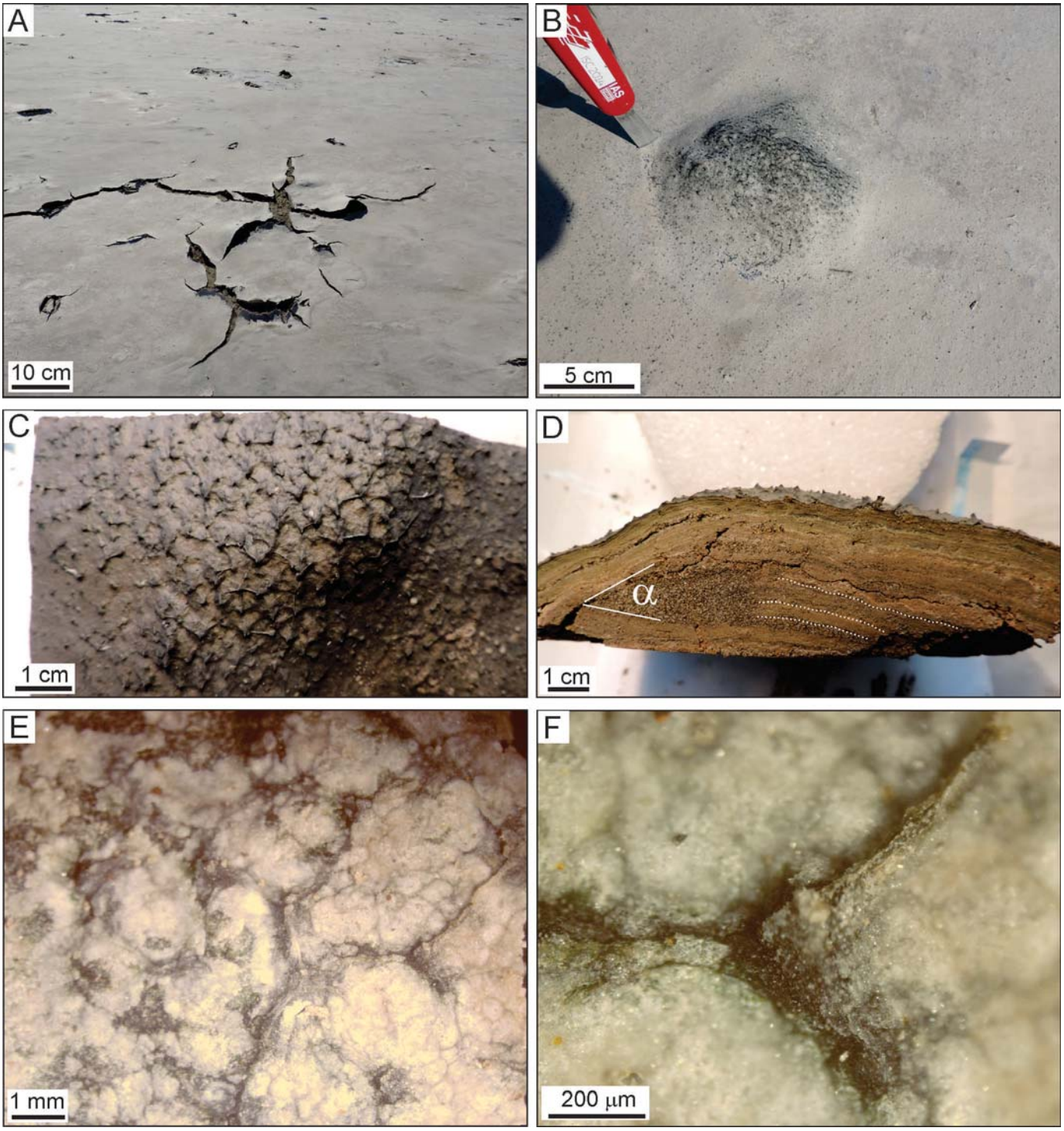

FIG. 6.—Later stages of pinnacle development under dry conditions. **A)** Typical appearance of the microbial surface with the formation of desiccation cracks. **B)** Gas dome covered by dense reticulate structures and **C)** surface in close-up view. **D)** Cross section of the dome in Part B; sand is entrapped under deformed top microbial layer that form an angle (α) with the microbial bottom layer. The profile shows the pinnacle formation at the surface of the microbial mat. **E)** Reticulate structures and pinnacles at high magnification. **F)** Close view of pinnacle or tuft structure formed by the junction of three reticulates.

diatoms were less abundant. The presence of pinkish sediment, even forming "aureolae" patterns on the mudflat surface is indicative of Archaea.

Under the microscope, the layered structure of pinnacles (Fig. 7A, B) was revealed to be composed of a densely packed mesh of parallel-oriented trichomes of *Phormidium* sp. that dominated the biomass of each pinnacle. Another conspicuous and abundant component of the community was *M. chthonoplastes*, while the cyanobacteria *Oscillatoria* sp., *Symploca* sp. and *Pseudanabaena* sp. were less abundant (Fig. 8). Pennate diatoms were also found as constituents of the pinnacles, in very low densities and thus

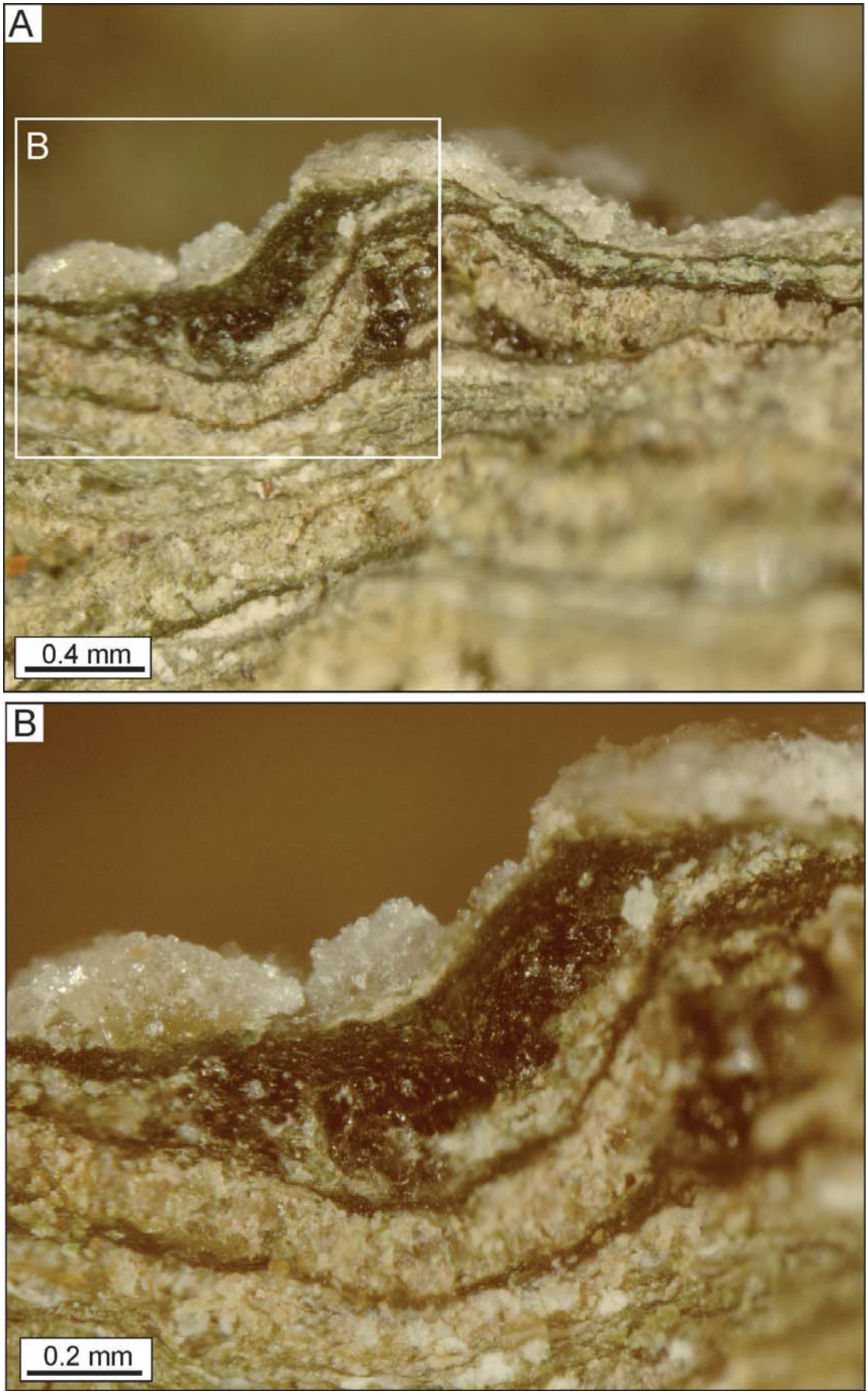
A
B
0.4 mm
B
0.2 mm

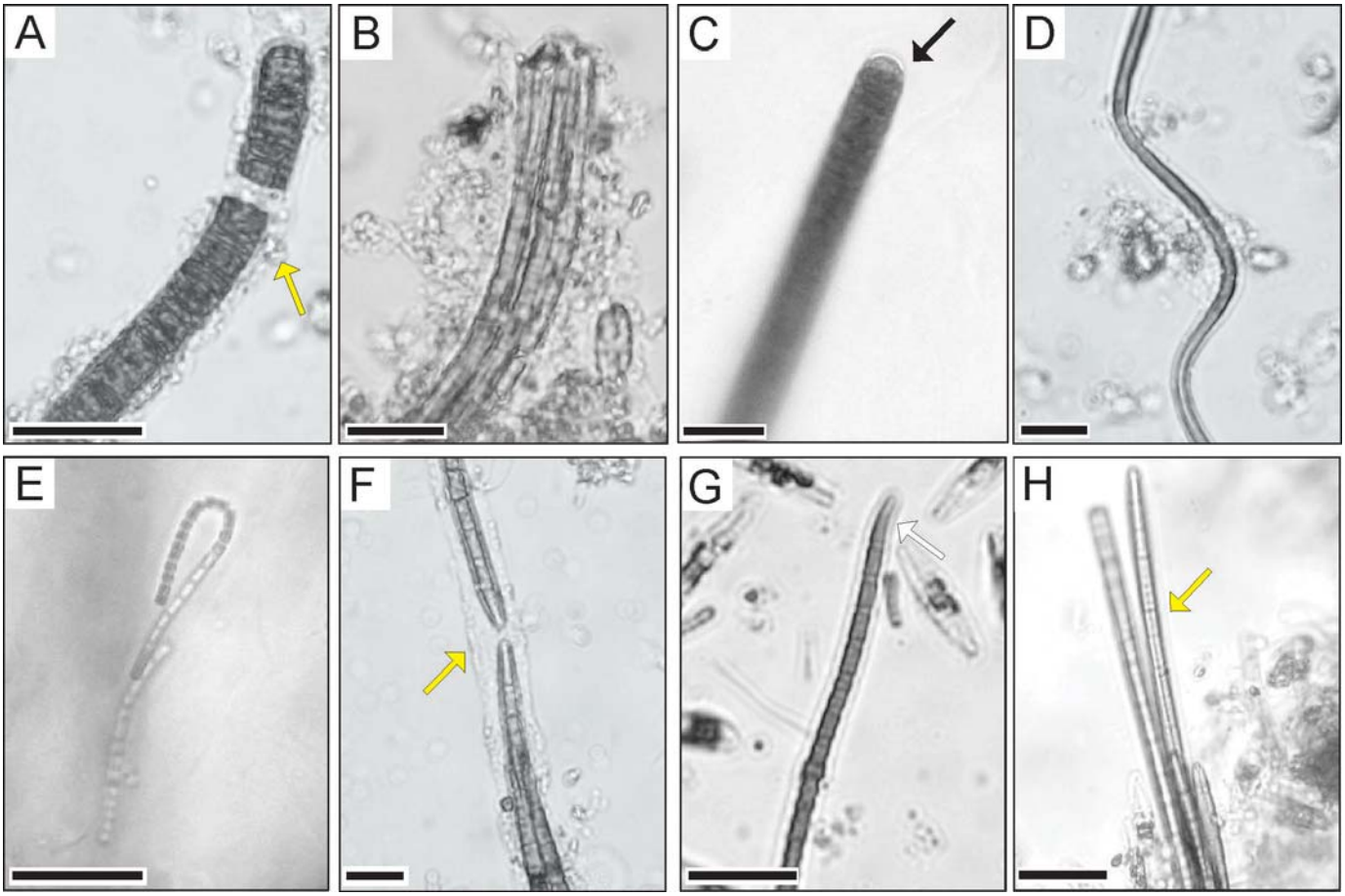

FIG. 8.—Light micrographs of oscillatorian cyanobacteria morphotypes found at Paso Seco. **A)** *Lyngbya* sp., showing the firm mucilaginous sheath surrounding each filament. **B)** *Microcoleus chthonoplastes* with mucilaginous sheath enveloping several densely packed, interwoven filaments and conical end cells. **C)** *Oscillatoria* sp. with calyptra on end cell. **D)** *Arthrospira* sp. with regularly screw-like coiling of trichome. **E)** *Pseudanabaena* sp. showing slight constrictions at cross walls. **F)** *Phormidium* sp. with mucilaginous sheath and pointed end cells. **G)** *Geitlerinema* sp. showing slight constriction at cross walls, and narrowed, slightly bent end cell. **H)** *Symploca* sp. filaments enveloped by thin sheath. Magnification 400 ×; scale bar = 10 μm.

contributing very little to the biomass; these were represented by *N. sigma*, *Amphora coffeaeformis*, *Diploneis* sp., and *Surirella* sp.

The observation of the cohesive highly hydrated mucilage with gelatinous consistency collected on 7/7/16 (see Fig. 5C) revealed an amorphous polysaccharide gel with embedded pennate diatoms under the microscope; *N. sigma* dominated the diatom biomass, and *C. closterium*, *Nitzschia* spp., *Navicula* sp., and *Amphora* sp. were also present. Chain-forming centric diatoms (*Melosira* sp.) and accessorial filamentous cyanobacteria such as *Pseudanabaena* sp. and *Oscillatoria* sp. were rare.

DISCUSSION

Several studies have described reticulates comparable to the ones in this study. Gerdes et al. (2000) and Gerdes (2007) described structures from the supratidal zone (sabkha) of Bahar Aluane, southern Tunisia, and concluded that their morphologies and size depended on the dominant cyanobacterium morphotype. In a similar area, on the Red Sea coastal plain, comparable reticulate structures with tufts and pinnacles were found in shallow pools of the intertidal and supratidal zones (Saudi Arabia, Taj et al. 2014; Abu Dhabi, Abed et al. 2008). In turn, Horodyski et al. (1977) provided a detailed description of the different mat morphologies that arise in relation to varying degrees of desiccation at Laguna Mormona, Mexico, and Horodyski (1977) later focused on *Lyngbya aestuarii*-dominated tufts in the same location. However, none of the above-mentioned studies focused on the evolution of these microbial structures.

Sediment colonized by microbial mats in the study site consists of characteristically porous sand, entrapping gases from the biological activity of microorganisms (often times presenting a laminated arrangement), old biolaminites, and gases probably entrapped by wave action over the tidal plain. The sequential evolution of reticulate morphologies documented during different seasons covers fluctuating solar radiation and storm-flooding conditions. There was a clear distinction between winter and summer seasons, which was reflected in the development and evolution of reticulate morphologies. During the winter, the frequent tidal flooding and sustained availability of water (Figs. 4A, 5A) promoted the creation of ephemeral shallow ponds, which were maintained for several days,

←

FIG. 7.—Cross section of dried-up cyanobacterial pinnacle. **A)** Planar lamination of the underlying microbial mat (dark lamina) showing its growth is apparent in the lower left of the photograph. The high density of cyanobacterial trichomes forms the core of the pinnacle. The mat grows by the processes of baffling and binding (Noffke 2010). **B)** Detail of the wavy laminar structure of the microbial mat with the high density of cyanobacteria forming the pinnacle.

TABLE 2.—*Mean linear dimensions (diameter; μm) measured on morphotypes of Oscillatorian cyanobacteria found at Paso Seco, with references to trichome gliding motility for strains within each genus. Filament sheaths are not included in measurements.*

Morphotype	Diameter (μm)	SE	n	reference to gliding motility
Pseudanabaena (trichome)	1.8	0.17	27	Shepard and Sumner (2010)
Geitlerinema (trichome)	2.3	0.03	20	Miller et al. (2012)
Arthrospira (trichome)	2.9	0.05	21	Fujisawa et al. (2010)
Phormidium (trichome)	3.7	0.10	20	Hoiczyk and Baumeister (1995)
Lyngbya (trichome)	4.1	0.18	20	Lamont (1969); Hoiczyk and Baumeister (1995)
Oscillatoria (trichome)	6.4	0.05	21	Lamont (1969); Hoiczyk and Baumeister (1995)
Symploca (fascicle)	6.5	0.39	22	Häder and Hoiczyk (1992)
M. chthonoplastes (fascicle)	7.9	0.23	20	Whale and Walsby (1984)

allowing microorganisms to colonize the surface substratum and form reticulates. In contrast, during spring and summer the intense solar radiation modified the evaporation budget of the plain, turning the mat whitish, and desiccation cracks became common microbial structures (arrow in Fig. 1B). Also, the drying-up of ponds facilitated preservation of reticulates and tufts after desiccation. Thus, our observations in Paso Seco corroborated the importance of environmental cues in the formation, modification, and preservation of reticulate structures. From our first record of reticulate structures in the field in October 2014 (Fig. 3), it became apparent that one essential condition for biofilm formation in Paso Seco is that a pre-established microbial mat must be covered by (a few centimeters of) calm water. This fact provides a medium for the surface-migrating trichomes to organize into reticulates. The prevalent mat type at the study site is typically cohesive and leathery in appearance, with elastic and flexible properties that are conferred by the thick, sheathed cyanobacterium *M. chthonoplastes* (Des Marais 2003; Kremer et al. 2008), which is dominant in terms of biomass. The initial formation of two-dimensional reticles is attributed to the two dominant species *M. chthonoplastes* and *Lyngbya* sp., which play a role in "seeding" the overlying fluid medium during flooding from the underlying, layered and compact mat, which has sufficient cell density to become suspended in the water column. Under calm conditions reticulate structures were formed on shallow ponds in a lapse from minutes to hours, depending on environmental conditions and cell density (Shepard and Sumner 2010).

All of the cyanobacteria found associated with reticulate geometries in this study (Fig. 8, Table 2) have been noted for their gliding motility. The collision of filaments determined by undirected motility is the mechanism responsible for aggregation and reticulate formation, as previously pointed out for laboratory cultures by Shepard and Sumner (2010). The mechanism implies trichomes coming into contact, then arranging into lines and determining bundles at the intersections (Fig 7), leaving the surrounding areas with lower cell density, thus creating a reticulate geometry that is preserved by desiccation (Fig. 6). The uneven distribution of ridges (Fig. 3A, B) indicates that under field conditions the cell density is non-uniform at this spatial scale. Compared to cell division and growth, cell motility is the most important factor for filaments to organize faster into reticulates (Gerdes 2007).

Interestingly, the arrangement of cyanobacteria in the early stages of reticulates consisting of trichomes of *Lyngbya* sp. at the surface is probably acting as a screening organism against adverse radiation wavelengths on top of *M. chthonoplastes*. The cyanobacterium *Lyngbya* sp. has the capacity to produce scytonemin, a pigment that provides a broad absorption in the UV and violet wavelengths, shielding *M. chthonoplastes* below (García-Pichel and Castenholz 1993). Moreover, these two cyanobacteria tolerate an air-dried state and complete dehydration for long periods through efficient repair of the DNA damage (Abed et al. 2008).

The gliding motility and tangling behavior of the mat-building filaments lead to tuft formation as the evolution of reticulates progresses. In later stages, *Phormidium* sp. and *M. chthonoplastes* become the most abundant and conspicuous cyanobacteria forming vertically condensed pinnacles. Tufts have been interpreted as indicative of microbial phototactic behavior (Shepard and Sumner 2010; Bosak et al. 2012; Sim et al. 2012; Reyes et al. 2013), and they may also represent a communal microbial strategy to penetrate the laminar boundary layer in the flowing medium above the substrate, gaining access to the overlying, nutrient-rich turbulent layer. The distribution pattern of pinnacles may be related to differences in nutrient concentration or space competition, while the bundles and tangles formed by the filaments produce a nonlinear growth pattern as a consequence of changes in the growth direction (Gerdes 2007). Consequently, tufts and pinnacles are formed by vertical movement and the reestablishment of cyanobacteria on the top of the mature mat surface (Fig. 7), as inferred by Tice et al. (2011).

The present field study emphasizes the importance of water conditions. Not only is shallow-water an important requirement for reticulate formation, but the temporal component is significant as well. When the flat was continuously inundated for longer periods (e.g., for at least 22 days by an $\sim$ 6.5-cm-high water column; see Fig. 5A), the growth of an extensive highly hydrated mucilage was promoted, failing to generate a reticulate morphology (Fig. 5C). On this occasion, the dominant microbes in this mucilage were eukaryotes (pennate diatoms) instead of cyanobacteria. Diatoms at high cell densities created a thick and transparent layer in close association, but were separated from the underlying mature mat by numerous bubbles (Fig. 5B), probably as a consequence of photosynthesizing cyanobacteria in the underlying mat. Another feature of this mucilage was the presence of calcite crystals (Fig. 5D), which might be induced by bacterial metabolism, in a way analogous to carbonate occurring beneath tufts as has been described by Gerdes et al. (2000).

Modern reticulate structures, which are the impression of entwined filamentous cyanobacteria, may give rise to wrinkle structures (Gerdes 2007) and elephant-skin textures (Gehling 1999), their fossil counterparts. In that context, the description of small-scale structures as reticulate patterns in modern mats lends support to the identification of ancient analogues. Pinnacles produce a nonlinear growth pattern that can be identified at the bounding planes in internal sequences of vertical sections of sedimentary stacks, and later in a sedimentary rock. In that sense, Simpson et al. (2013, their Fig. 12), Noffke et al. (2013), and Homann et al. (2015) found reticulate structures in Precambrian (3.22 Ga old) continental rocks from South Africa, studying polished sandstone slabs. However, these wrinkle structures were interpreted as upper-intertidal-zone to supratidal-zone features, subject to moderate water agitation. Shepard and Sumner (2010, and references therein) mentioned the importance of low flow speeds in order to maintain the reticulate structures attached to a substrate. Likewise, the hydrodynamic regime associated with the presence

FIG. 9.—Microbial deformed structures (MDS *sensu* Bouougri and Porada 2012) in Paso Seco, indicative of high-energy hydrodynamic regimes. **A)** Rip-off mat and fold-over sedimentary structures; the surface mat shows a coriaceous aspect being desiccated by solar radiation. **B)** Detached mat fragment deformed by water current during inundation; it looks like a piece of flexible and cohesive cloth made stiff by desiccation. **C)** Roll-up microbial sedimentary structure. **D)** Fold microbial structure formed when the thick microbial mat slides over the underlying sediment. See Cuadrado et al. (2015) for further details.

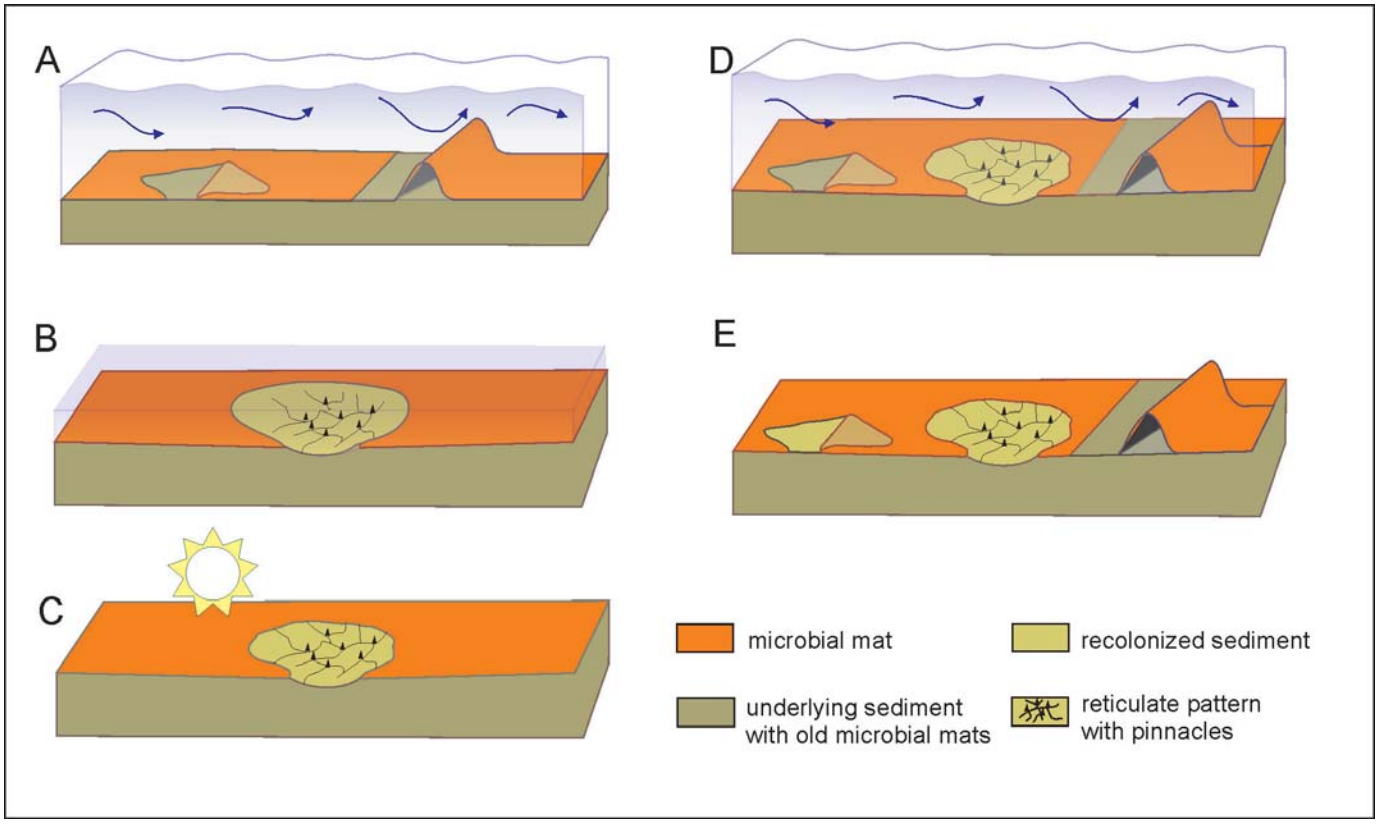

FIG. 10.—Schematic diagram showing the evolution of reticulate structures in microbial mats. **A)** High-energy flooding generating MDS such as microbial folds and flipped-over edge mats. **B)** Formation of delicate reticulate structures and pinnacles in an erosional pocket under a shallow lamina of water during calm conditions. **C)** Dehydration and desiccation of the microbial structures by solar radiation. **D)** Subsequent high-energy flooding events act over the desiccated reticulate structures. **E)** Co-occurring deformed sedimentary structures and reticulate patterns in microbial mats.

of reticulate structures in coastal settings is commonly related to low energy (Gehling 1999).

On the other hand, due to the shape of the studied area (a paleo-tidal channel) the volume of the flooding (which occurs only under storm conditions) is constrained in the zone making a fast-moving current. Thus, deformed microbial sedimentary structures such as ripped mats, folds and roll-ups are formed (Fig. 9; and further details in Cuadrado et al. 2015). Therefore, Paso Seco is considered as a high-energy sedimentary environment with times of calm conditions when microbial mats can develop. This aspect allows us to differentiate between how the reticulate microbial structures behave when subjected to different energy levels. We documented the occurrence of delicate reticulate structures formed after flooding (Fig. 3A), and also stiff- and darker-looking pinnacles and polygonal ridges as examples of permanent structures preserved after solar-induced desiccation (Fig. 6C) that withstand high energy. The schematic diagram in Figure 10 shows significant steps in the evolution of the reticulate pattern. Our study confirms that monitoring the evolution over time of microbial structures in modern settings contributes to the reconstruction of both paleoenvironmental parameters and the paleomicrobenthos in fossil structures (Noffke 2010).

CONCLUSION

This study followed the sequential evolution of reticulate microbial structures formed by dominant motile cyanobacteria, on top of an existing layered and compact microbial mat. The study area is characterized by pulses of hydrodynamic energy alternating with calm periods; thus the evolutionary stages of reticulate microbial structures could be evaluated under both. Reticulate patterns develop as delicate structures under a lamina of calm water after an inundation, and ultimately create three-dimensional protruding tufts and pinnacles in junctional positions after their desiccation by solar radiation and dehydration. These firm microbial reticulates can withstand intermittent high-energy hydrodynamic regimes that are also responsible for the formation of co-occurring deformed sedimentary structures. We conclude that it is misleading to strictly relate the origin of reticulate structures to calm conditions, since they can withstand high-energy pulses after their desiccation.

When studying the geological record it is important to look for various lines of evidence to confirm the inferred hydrodynamic regime associated with such structures. Consequently, our contribution raises a cautionary note for the interpretation of the hydrodynamic environment where reticulate microbial structures are present.

ACKNOWLEDGMENTS

The authors acknowledge the collaboration of E.A. Gómez, L. Maisano, I.E. Quijada, and L.A. Raniolo during field work. This project was funded by grants PICT 2012-309 from Agencia Nacional de Promocion Científica y Tecnologica, PIP 2013 No. 4061 from Consejo Nacional de Investigación Científica y Tecnológica (CONICET), and PGI 24/H138 from Secretaría de Ciencia y Tecnología de la Universidad Nacional del Sur (awarded to DGC). We thank Matthew Stimson, Brian Pratt, Nora Noffke, and Prof. Gingras as Associate Editor for constructive comments that improved the quality of the manuscript.

REFERENCES

Abed, R.M.M., Kohls, K., Schoon, R., Scherf, A.-K., Schacht, M., Palinska, K.A., Al-Hassani, H., Hamza, W., Rullkötter, J., and Golubic, S., 2008, Lipid biomarkers, pigments and cyanobacterial diversity of microbial mats across intertidal flats of the arid coast of the Arabian Gulf (Abu Dhabi, UAE): FEMS Microbiology Ecology, v. 65, p. 449–462.

Blakemore, L.C., Searle, P.L., and Daly, B.K., 1987, Methods for chemical analysis of soils: New Zealand Soil Bureau, Scientific Report, 80 p.

Blott, S.J., and Pye, K., 2001, Gradistat: a grain size distribution and statistics package for the analysis of unconsolidated sediments: Earth Surface Processes and Landforms, v. 26, p. 1237–1248.

Bosak, T., Liang, B., Wu, T.D., Templer, S.P., Evans, A., Vali, H., Guerquin-Kern, J.L., Klepac-Ceraj, V., Sim, M.S., and Mui, J., 2012, Cyanobacterial diversity and activity in modern conical microbialites: Geobiology, v. 10, p. 384–401.

Bouougri, E.H., and Porada, H., 2012, Wind-induced mat deformation structures in recent tidal flats and sabkhas of SE-Tunisia and their significance for environmental interpretation of fossil structures: Sedimentary Geology, v. 263–264, p. 56–66.

Churro, C., Valério, E., Vieira, L., Pereira, P., and Vasconcelos, V., 2016, Evaluation of methanol preservation for molecular and morphological studies in cyanobacteria using *Planktothrix agardhii*: Journal of Applied Phycology, v. 28, 1713–1723.

Cuadrado, D.G., Pan, J., Gómez, E.A., and Maisano, L., 2015, Deformed microbial mat structures in a semiarid temperate coastal setting: Sedimentary Geology, v. 325, p. 106–118.

Des Marais, D.J., 2003, Biogeochemistry of hypersaline microbial mats illustrates the dynamics of modern microbial ecosystems and the early evolution of the Biosphere: Biological Bulletin, v. 204, p. 160–167.

Espinosa, M.A., and Isla, F.I., 2011, Diatom and sedimentary record during the mid-Holocene evolution of the San Blas estuarine complex, northern Patagonia, Argentina: Ameghiniana, v. 48, p. 411–423.

Flannery, D.T., and Walter, M.R., 2012, Archean tufted microbial mats and the Great Oxidation Event: new insights into an ancient problem: Australian Journal of Earth Sciences, v. 59, p. 1–11.

Fujisawa, T., Narikawa, R., Okamoto, S., Ehira, S., Yoshimura, H., Suzuki, I., Masuda, T., Mochimaru, M., Takaichi, S., Awai, K., Sekine, M., Horikawa, H., Yashiro, I., Omata, S., Takarada, H., Katano, Y., Kosugi, H., Tanikawa, S., Ohmori, K., Sato, N., Ikeuchi, M., Fujita, N., and Ohmori, M., 2010, Genomic structure of an economically important cyanobacterium, Arthrospira (Spirulina) platensis NIES-39: DNA Research dsq004, p. 1–19.

García-Pichel, F., and Castenholz, R.W., 1993, Occurrence of UV-absorbing, mycosporine-like compounds among cyanobacterial isolates and an estimate of their screening capacity: Applied and Environmental Microbiology, v. 59, p. 163–169.

Gehling, J., 1999, Microbial mats in terminal Proterozoic siliciclastics: Ediacaran death masks: Palaios, v. 14, p. 40–57.

Gerdes, G., 2007, Structures left by modern microbial mats in their host sediments, *in* Schieber, J., Bose, P.K., Eriksson, P., Banerjee, S., Sarkar, S., Altermann, W., and Catuneanu, O., eds., Atlas of Microbial Mat Features Preserved within the Siliciclastic Rock Record: Amsterdam, Elsevier, p. 5–38.

Gerdes, G., Klenke, T., and Noffke, N., 2000, Microbial signatures in peritidal siliciclastic sediments: a catalogue: Sedimentology, v. 47, p. 279–308.

Häder, D., and Hoiczyk, E., 1992, Gliding motility, *in* Melkonian, M., ed., Algal Cell Motility: New York, Chapman and Hall, p. 1–38.

Hagadorn, J.W., and Bottjer, D.J., 1997, Wrinkle structures: microbially mediated sedimentary structures common in subtidal siliciclastic settings at the Proterozoic–Phanerozoic transition: Geology, v. 25, p. 1047–1050.

Hoiczyk, E., and Baumeister, W., 1995, Envelope structure of four gliding filamentous cyanobacteria: Journal of Bacteriology, v. 177, p. 2387–2395.

Homann, M., Heubeck, C., Airo, A., and Tice, M.M., 2015, Morphological adaptations of 3.22 Ga-old tufted microbial mats to Archaean coastal habitats (Moodies Group, Barberton Greenstone Belt, South Africa): Precambrian Research, v. 266, p. 47–64.

Horodyski, R.J., 1977, *Lyngbya* mats at Laguna Mormona, Baja California, Mexico: comparison with Proterozoic stromatolites: Journal of Sedimentary Petrology, v. 47, p. 1305–1320.

Horodyski, R.J., Bloeser, B., and Vonder Haar, S., 1977, Laminated algal mats from a coastal lagoon, Laguna Mormona, Baja California, Mexico: Journal of Sedimentary Petrology, v. 47, p. 680–696.

Komárek, J., and Hauer, T., 2013, CyanoDB.cz: on-line database of cyanobacterial genera: World-wide electronic publication, University of South Bohemia and Institute of Botany, http://www.cyanodb.cz.

Kremer, B., Kazmerczak, J., and Stal, L.J., 2008, Calcium carbonate precipitation in cyanobacterial mats from sandy flats of the North Sea: Geobiology, v. 6, p. 46–56.

Lamont, H.C., 1969, Shear-oriented microfibrils in the mucilaginous investments of two motile oscillatoriacean blue-green algae: Journal of Bacteriology, v. 97, p. 350–361.

Miller, A.W., Blackwelder, P., Al-Sayegh, H., and Richardson, L.L., 2012, Insights into migration and development of coral black band disease based on fine structure analysis: Revista de Biología Tropical, v. 60, p. 21–27.

Noffke, N., 2010, Microbial Mats in Sandy Deposits from the Archean Era to Today: Berlin, Springer-Verlag, 166 p.

Noffke, N., Gerdes, G., Klenke, T., and Krumbein, W.E., 2001, Microbially induced sedimentary structures: a new category within the classification of primary sedimentary structures: Journal of Sedimentary Research, v. 71, p. 649–656.

Noffke, N., Beukes, N., Bower, D., Hazen, R.M., and Swift, D.J., 2008, An actualistic perspective into Archean worlds: (cyano-)bacterially induced sedimentary structures in the siliciclastic Nhlazatse Section, 2.9 Ga Pongola Supergroup, South Africa: Geobiology, v. 6, p. 5–20.

Noffke, N., Christian, D., Wacey, D., and Hazen, R.M., 2013, Microbially induced sedimentary structures recording an ancient ecosystem in the ca. 3.48 billion-year-old Dresser Formation, Pilbara, Western Australia: Astrobiology, v. 13, p. 1103–1124.

Park, R.K., 1977, The preservation potential of some recent stromatolites: Sedimentology, v. 24, p. 485–506.

Petroff, A.P., Sim, M.S., Maslov, A., Krupenin, M., Rothman, D.H., and Bosak, T., 2010, Biophysical basis for the geometry of conical stromatolites: National Academy of Sciences (USA), Proceedings, v. 107, p. 9956–9961.

Reyes, K., Gonzalez, N.I., Stewart, J., Ospino, F., Nguyen, D., Cho, D.T., Ghahremani, N., Spear, J.R., and Johnson, H.A., 2013, Surface orientation affects the direction of cone growth by *Leptolyngbya* sp., Strain C1, a likely architect of coniform structures Octopus Spring (Yellowstone National Park): Applied and Environmental Microbiology, v. 79, p. 1302–1308.

Round, F.E., Crawford, R.M., and Mann, D.G., 1990, The Diatoms: Biology and Morphology of the Genera: Cambridge UK, Cambridge University Press, 747 p.

Shepard, R.N., and Sumner, D.Y., 2010, Undirected motility of filamentous cyanobacteria produces reticulate mats: Geobiology, v. 8, p. 179–190.

Sim, M.S., Liang, B., Petroff, A.P., Evans, A., Klepac-Ceraj, V., Flannery, D.T., Walter, M.R., and Bosak, T., 2012, Oxygen-dependent morphogenesis of modern clumped photosynthetic mats and implications for the Archean stromatolite record: Geosciences, v. 2, p. 235–259.

Simpson, E.L., Heness, E., Bumby, A., Eriksson, P.G., Eriksson, K.A., Hilbert-Wolf, H.L., Linnevelt, S., Malenda, H.F., Modungwa, T., and Okafor, O., 2013, Evidence for 2.0 Ga continental microbial mats in a paleodesert setting: Precambrian Research, v. 237, p. 36–50.

Sumner, D.Y., 1997, Late Archean calcite–microbe interactions: two morphologically distinct microbial communities that affected calcite nucleation differently: Palaios, v. 12, p. 300–316.

Sumner, D.Y., 2000, Microbial versus environmental influences on the morphology of Late Archean fenestrate microbialites, *in* Riding, R.E., and Awramik, S.M., eds., Microbial Sediments: Berlin, Springer-Verlag, p. 307–314.

Taj, R., Aref, M.A., and Schreiber, B.C., 2014, The influence of microbial mats on the formation of sand volcanoes and mounds in the Red Sea coastal plain, south Jeddah, Saudi Arabia: Sedimentary Geology, v. 311, p. 60–74.

Tice, M.M., Thornton, D.C.O., Pope, M.C., Olszewski, T.D., and Gong, J., 2011, Archaean microbial mat communities: Annual Review of Earth and Planetary Sciences, v. 39, p. 297–319.

Waterbury, J.B., 2006, The Cyanobacteria: isolation, purification and identification, *in* Dworkin, M., Falkow, S., Rosenberg, E., Schleifer, K.H., and Stackebrandt, E., eds., The Prokaryotes, a Handbook on the Biology of Bacteria, Third Edition: New York, Springer, p. 1053–1073.

Whale, G.F., and Walsby, A.E., 1984, Motility of the cyanobacterium *Microcoleus chthonoplastes* in mud: British Phycological Journal, v. 19, p. 117–123.

Received 15 February 2017; accepted 30 October 2017.